Separation Science and Technology
Publication details, including instructions for authors and subscription information:
http://www.informaworld.com/smpp/title~content=t713708471

Thermodynamic and Kinetic Study of Adsorption of R,S-α-Tetralol Enantiomers on the Chiral Adsorbent CHIRALPAK AD

Michal Zabka[a]; Alírio E. Rodrigues[a]
[a] Laboratory of Separation and Reaction Engineering (LSRE), Department of Chemical Engineering, Faculty of Engineering, University of Porto, Porto, Portugal

To cite this Article Zabka, Michal and Rodrigues, Alírio E.(2007) 'Thermodynamic and Kinetic Study of Adsorption of R,S-α-Tetralol Enantiomers on the Chiral Adsorbent CHIRALPAK AD', Separation Science and Technology, 42: 4, 739 — 768
To link to this Article: DOI: 10.1080/01496390601120706
URL: http://dx.doi.org/10.1080/01496390601120706

Separation Science and Technology, 42: 739–768, 2007

ISSN 0149-6395 print/1520-5754 online
DOI: 10.1080/01496390601120706

Thermodynamic and Kinetic Study of Adsorption of R,S-α-Tetralol Enantiomers on the Chiral Adsorbent CHIRALPAK AD

Michal Zabka and Alírio E. Rodrigues
Laboratory of Separation and Reaction Engineering (LSRE), Department of Chemical Engineering, Faculty of Engineering, University of Porto, Porto, Portugal

Abstract: Experimental results for the separation of S,R-α-Tetralol enantiomers obtained on preparative columns packed with particle size 20 μm of chiral adsorbent CHIRALPAK AD are presented. The total porosity was measured by using the non-retained compound 1,3,5-Tri-tert-butylbenzene and was 0.61. The permeability of the bed packed with CHIRALPAK AD was calculated as 4.4×10^{-13} m^2. The efficiency of columns was characterized by the height equivalent to a theoretical plate (HETP) and a linear dependency has been found over tested flow rates. The HETP of S-α-Tetralol and R-α-Tetralol calculated at the flow rate 5.0 cm^3/min were 320 μm and 340 μm, respectively. Thermodynamic adsorption parameters enthalpy, ΔH and entropy, ΔS, have been calculated from van't Hoff plot. Equilibrium and kinetics of adsorption of single enantiomers and racemic mixture of α-Tetralol on CHIRALPAK AD were evaluated as well. The parameters for multicomponent isotherm linear-Langmuir model are presented. The breakthrough curves of α-Tetralol enantiomers are simulated with a mathematical model that accounts for axial dispersion and linear driving force for the intraparticle mass transfer.

Keywords: Chiralpak AD, liquid chromatography, hydrodynamic characterization, mathematical modeling, chiral alcohol, chiral separation

Received 1 September 2006, Accepted 8 November 2006

Address correspondence to Alírio E. Rodrigues, Laboratory of Separation and Reaction Engineering (LSRE), Department of Chemical Engineering, Faculty of Engineering, University of Porto, Rua Dr. Roberto Frias s/n, 4200-465, Porto, Portugal. Tel.: 351 22 5081671; Fax: 351 22 5081674; E-mail: arodrig@fe.up.pt

INTRODUCTION

Evidence of the stereochemistry in metabolism path and pharmacokinetics of drugs has become an issue for the pharmaceutical industry. It is well known that the pharmacologically inactive enantiomer can show unwanted side effects, antagonistic or toxic effects. Therefore, separation of pure enantiomers is becoming one of the most challenging issues. During the last decades there has been an interest in the development of efficient, economical, and simple methods in the production of pure enantiomers products on the analytical or preparative level (1–3).

In preparative chromatography, throughput is defined as the amount of purified material per unit of time and per unit of mass of stationary phase. Different factors affect throughput, namely, the loading capacity of the chiral stationary phases, column efficiency, selectivity, temperature, column size, flow rate, feed concentration, which itself depends on the solubility of the solute.

Most of the chiral selectors are obtained from natural and synthetic sources. Derivatized amyloses and derivatized celluloses as chiral stationary phases have promising chiral recognition properties and high loading capacity (3, 4). Nowadays, immobilized versions of amylose and cellulose tris(3,5-dimethylphenylcarbamate) are available which offer compatibility with a wide range of organic solvents and the enhancement of enantioseparation on the chiral stationary phase (5–7). Examples are amylose tris(3,5-dimethylphenylcarbamate) and cellulose tris(3,5-dimethylphenylcarbamate). Both chiral stationary phases consist of tris(3,5-dimethylphenylcarbamate)-D-glucose units as chiral adsorbing sites and are offering a great versatility for separating a wide range of chiral compounds. The objectives of this work are to investigate hydrodynamic and sorption properties of the preparative column packed with chiral adsorbent CHIRALPAK AD with particle diameter 20 μm. The mobile phase dependence of the height equivalent to a theoretical plate (HETP) was determined, to acquire the kinetic data of the chiral adsorbent CHIRALPAK AD.

The methodology includes the following:

a. Elution chromatography experiments with non-adsorbed species on the chiral adsorbent CHIRALPAK AD to evaluate the void volume of the column.
b. Elution chromatography experiment with the enantiomers of R,S-α-Tetralol on the chiral adsorbent CHIRALPAK AD to determine the mobile phase velocity dependence of the height equivalent to the plate for each pure enantiomer. Study of thermodynamics of adsorption of R,S-α-Tetralol enantiomers on the chiral adsorbent CHIRALPAK AD were performed.
c. Measurements of the competitive isotherms by frontal chromatography experiments with the racemate of R,S-α-Tetralol on the chiral adsorbent CHIRALPAK AD were performed.

d. Measurements of the single isotherms by frontal chromatography experiments with the pure enantiomers of R,S-α-Tetralol on the analytical column filled by chiral adsorbent CHIRALPAK AD were performed.

THEORETICAL

The mathematical model used to describe the dynamic behavior of the fixed bed adsorber considers the following assumptions: the axial dispersed plug flow model describes the fluid flow; external and internal mass-transfer resistance for adsorbable species is combined in an overall mass transfer coefficient; isothermal process; constant column length and packing porosity.

The model equations (8, 9) are established by the following system of mass balance for species i in the mobile phase of the column bed and in the adsorbent particle, where C_i is the concentration in the bulk fluid, $\bar{C}_{pi}$ is the average concentration in the particle pores and q_i is the adsorbed phase concentration in equilibrium with C_{pi}, $\bar{q}_i$ is average adsorbed phase concentration in particle.

Mass balance of component i in the bulk fluid:

$$\frac{\partial C_i}{\partial t} + v\frac{\partial C_i}{\partial z} = D_L\frac{\partial^2 C_i}{\partial z^2} - \frac{1-\varepsilon}{\varepsilon}k_{ov}a_p(C_i - \bar{C}_{pi}) \tag{1}$$

Mass balance of species i in adsorbent:

$$\varepsilon_p\frac{\partial \bar{C}_{pi}}{\partial t} + \frac{\partial \bar{q}_i}{\partial t} = k_{ov}a_p(C_i - \bar{C}_{pi}) \tag{2}$$

Multicomponent adsorption equilibrium isotherm:

$$q_i = f(C_{p,i}) \tag{3}$$

The initial condition is:

$$\mathrm{t} = 0,\ C_i = \bar{C}_{pi} = \bar{q}_i = 0 \tag{4}$$

The Danckwerts boundary conditions at the column inlet (z = 0) and column exit (z = L) for $t > 0$ are:

$$\mathrm{z} = 0, \quad D_L\frac{\partial C_i}{\partial z} = v(C_0 - C_i) \tag{5}$$

$$\mathrm{z} = \mathrm{L}, \quad \frac{\partial C_i}{\partial z} = 0 \tag{6}$$

where v is the interstitial velocity, D_L is the axial dispersion coefficient, ε and ε_p are the bed and particle porosity, respectively, k_{ov} is the overall mass transfer coefficient, a_p is the specific surface area of the adsorbent particle.

The overall mass transfer coefficient is given by (10, 11)

$$k_{ov} = \frac{1}{1/k_{ext} + 1/k_{int}} \tag{7}$$

where k_{ext} and k_{int} are the external (film) and internal mass transfer coefficient. As an approximation the expression suggested by Glueckauf has been used and is given by

$$k_{\text{int}} = \frac{10 D_{pe}}{d_p} \tag{8}$$

where $D_{pe} = \varepsilon_p D_m / \tau$ is pore diffusivity, D_m molecular diffusivity, and τ is tortuosity factor, d_p is the particle size. The tortuosity factor was estimated by

$$\tau = \frac{(2 - \varepsilon_p)^2}{\varepsilon_p} \tag{9}$$

The external (film) mass transfer coefficient, k_{ext}, was calculated (9) by:

$$Sh = \frac{k_{ext} d_p}{D_m} = \frac{1.09}{\varepsilon} (Sc\text{Re})^{1/3} \tag{10}$$

where $Sc = \eta / \rho D_m$ is the Schmidt number and $\text{Re} = \rho v \varepsilon d_p / \eta$ is the Reynolds number.

Two main mechanisms are lumped in the axial dispersion coefficient: molecular diffusion and eddy diffusion (12). As a first guess the axial dispersion coefficient is given by

$$D_L = \gamma_1 D_m + \gamma_2 d_p v \tag{11}$$

where γ_1, γ_2 are constants ($\gamma_1 = 20/\varepsilon$ and $\gamma_2 = 0.5$). However, as it will be shown on the influence of the interstitial velocity upon the equivalent height of a theoretical plate, the contribution of molecular diffusion to axial dispersion is negligible and therefore one can write

$$D_L = \gamma_2 d_p v \tag{12}$$

The molecular diffusivities of the adsorbate were calculated by the Wilke–Chang equation (13) and extended to mixed solvents by Perkins and Geankoplis (14):

$$D_m = 7.4 \times 10^{-8} \frac{T\sqrt{\phi M}}{\eta V_m^{0.6}} \tag{13}$$

where $T(K)$ is the absolute temperature, η its viscosity (cP), which was calculated according to Teja and Rice method for liquid mixture (15).

The term ϕM is given by: $\phi M = x_A \phi_A M_A + x_B \phi_B M_B$ where x_A, x_B are the molar fractions, the association factors ϕ_A, ϕ_B are constants, which account for solute-solvent interactions ($\phi_A = \phi_B = 1$), and the molar mass M_A, M_B

(g/mol) of the single components A and B of the mixed solvent. The molar volume of the adsorbate V_m (cm^3/mol) at its normal boiling temperature was estimated by Le Bas method (16).

Model equations (Eq. 1–6) were solved with gPROMS package (17). The mathematical model involves a system of partial and algebraic equations (PDAEs). The axial domain was discretized by using orthogonal collocation method in finite elements (OCFEM); third order polynomials were used in the 40 elements. The system of ordinary differential and algebraic equation (ODAEs) was integrated over time using the DASOLV integrator implemented in gPROMS. For all simulations a tolerance equal to 10^{-5} was fixed.

EXPERIMENTAL

Equipment

Elution experiments were performed on Gilson 712 HPLC system equipped with HPLC pumps model 305 and 306, manual injector Rheodyne with the injection loop 500 μl and UV detector model 115 ($\lambda = 270$ nm). Gilson 712 HPLC software was used for data acquisition and control.

Materials and Chemicals

CHIRALPAK AD (amylose tris(3,5-dimethylphenyl carbamate)) coated on a 20 μm silica gel substrate was used as chromatographic media supplied by Chiral Technologies Europe, France. The basic physical-chemical properties are listed in Table 1. The structural unit of the packing composition is shown in Fig. 1. Chiral adsorbent was characterized by SEM analysis presented in Fig. 2.

Superformance preparative columns (Merck, German) with adjustable length, 26-mm I.D. were used in all experiments. The external porosity of the preparative column was assumed equal to 0.4 and the total porosity was

Table 1. Physico – chemical properties of the chiral adsorbent CHIRALPAK AD – 20 μm supplied by the manufacturer

Parameters	Specification
Appearance	white, off-white powder
Pore size	1500 ± 400 Å
Carbon content	$14\% \leq C \leq 16\%$
Loss on drying	not more than 1.5 wt%

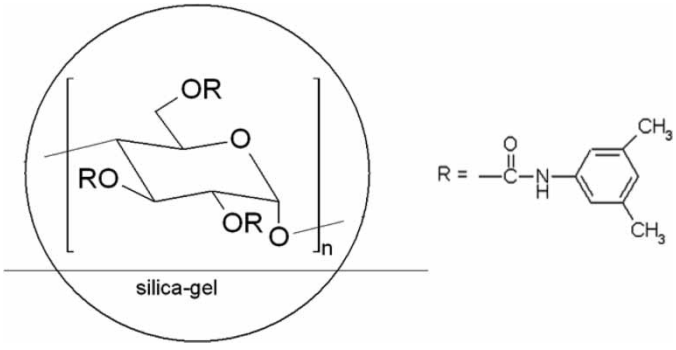

Figure 1. The structural unit of the chiral adsorbent CHIRALPAK AD.

evaluated by injecting the polar non-retained compound 1,3,5-Tri-tert-butylbenzene. The procedure used to calculate the values of the total porosities of the prepared columns is described later.

For the experiments were used 1,3,5-Tri-tert-butylbenzene (TTBB), minimum 97.0 % purity purchased from Sigma-Aldrich Chemie, Germany, R,S-(±)-1,2,3,4-Tetrahydro-1-naphthol (R,S-α-Tetralol) minimum 99% purity, purchased from Fluka Chemie, Switzerland.

The mobile phase used was n-Heptane/2-propanol (95/5). The n-Heptane ($\geq$99.8%) and 2-propanol (per analysis purity) were purchased from Fluka Chemie (Buchs, Switzerland).

All solutions of the tested compounds were prepared in the mobile phase. The solutions were used after degassing following filtration on 0.2 μm, 50 mm in diameter NL 16-membrane filter (Schleicher & Schuell, Germany) for all elution chromatography experiments.

Packing Procedure of the Preparative Column

CHIRALPAK AD (amylose tris(3,5-dimethylphenyl carbamate)) coated on a 20-μm silica gel substrate used as stationary phase was added to n-hexane and degassed under vacuum with occasional mechanical mixing of a suspension. The adsorbent has been taken under vacuum for approximately two hours to replace all air from the pores of the adsorbent.

The packing procedure, proposed by Nicoud (18), has been used to fill the preparative column with chiral adsorbent. The column was filled slowly with the prepared suspension of solvent and adsorbent. The filled column was closed very carefully and the bed was compacted with n-hexane/2-propanol (90/10) at a flow rate 40 cm^3/min. After this step, the backpressure regulator has been closed step by step up to the pressure at the outlet of the column increased to 30 bars. The packing procedure has been finished when

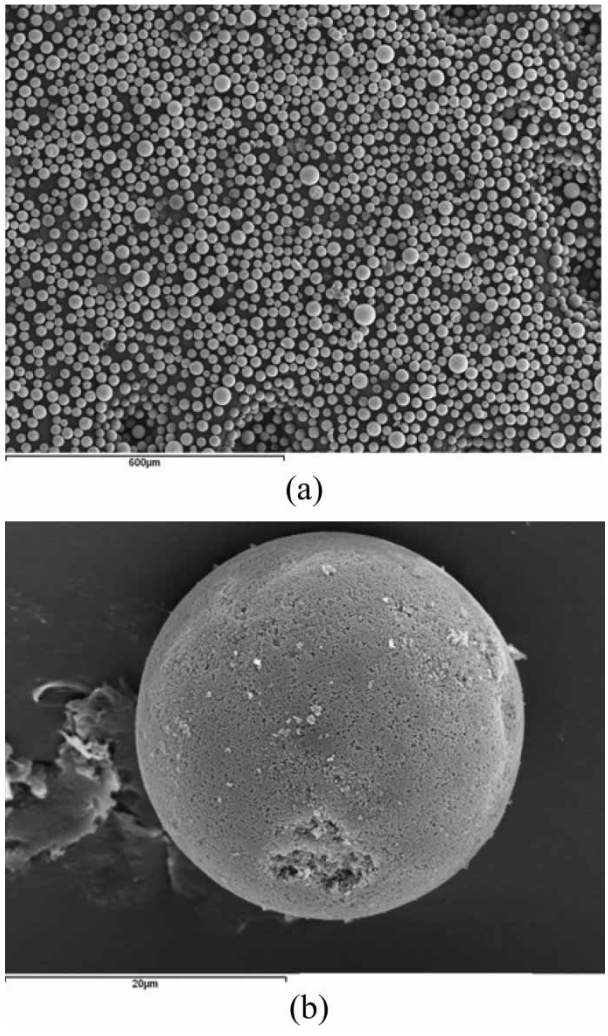

Figure 2. SEM microphotographs of the silica gel support with particle size 20 µm: (a) under 100 X magnification scale 600 µm (b) under 3000 X magnification scale 20 µm

the required length of the bed was achieved. Finally, the piston position was carefully adjusted, without crushing the phase near the bed surface, to avoid any dead volume.

At the end of each experiment the chiral columns was always flushed with five and more column volumes of the recommended hexane/2-propanol (90/10) storage solvent. The procedure is to preserve the lifetime of the chiral adsorbent and minimize any possible irreversible interaction of the chiral adsorbent with components in the mobile phase.

Elution Chromatography Experiments

This experimental section was divided into two parts. The first part was used to carry out the hydrodynamic characterization of column filled with CHIRALPAK AD with particle size 20 μm. The total porosity was evaluated by injecting the solution of the non-retained compound, 1,3,5-Tri-tert-butylbenzene. The second part of the elution experiment was carried out to measure the column efficiency for 1,3,5-Tri-tert-butylbenzene and each pure enantiomer of R,S-α-Tetralol. The concentration was 0.5 g/dm^3 in all cases of tested substances. The mobile phase n-Heptane/2-propanol (95/5, v/v) was used. Each compound was dissolved in the prepared mobile phase. An amount of 500 μl of the sample solution was injected into the column through which the mobile phase was flowing. Pulse experiments were conducted in the range of flow rates from 5.0 cm^3/min to 40 cm^3/min. The measurements were acquired at a wavelength of UV detector $\lambda = 270$ nm. All experiments were carried out at constant temperature (25°C) and pressure drops were measured for each run.

Frontal Chromatography Experiments

The frontal analysis technique (FA) (9) was used for determination of the competitive adsorption equilibrium isotherm of R,S-α-Tetralol on the preparative column packed with CHIRALPAK AD. One pump was transferring the sample solution through the column until the outlet concentration had reached the inlet concentration; afterwards the second pump was used to deliver the solution of the mobile phase and the eluted volume resulting from the desorption step was collected and analyzed. Subsequently the whole system was re-equilibrated with pure mobile phase. The temperature of the system was controlled by a thermostatic bath. All measurements were carried out at constant temperature (25°C) and at a flow rate of 5 cm^3/min. Mobile phase used was the mixture of n-Heptane/2-propanol (95/5). The FA measurements were acquired at a wavelength (λ) of 270 nm. A range of the racemate concentration from 1 to 16 g/dm^3 was used.

Single adsorption equilibrium isotherm measurement on the analytical column (25 × 0.46 cm, I.D.) packed with chiral adsorbent CHIRALPAK AD has been performed. All measurements have been performed by the same procedure as mentioned above. The range of the feed concentration was from 1 to 10 g/dm^3 for each solution enantiomer. Single adsorption equilibrium isotherm of enantiomers at ambient temperature (≈25°C) and at a flow rate 1 cm^3/min was obtained. The solvent and mobile phase was the same as in the case of the measurement of competitive isotherm.

RESULTS AND DISCUSSION

Hydrodynamic Study of the Chiral Preparative Column

Elution chromatography experiments with non-retained species were performed to determine the total porosity of the column, the influence of the flow rate upon height equivalent to a theoretical plate and permeability of the preparative chiral column filled with CHIRALPAK AD.

The total porosity of the column is defined as follows:

$$\varepsilon_T = \frac{V_T}{V} = \frac{t_R Q}{V} \tag{14}$$

where V_T is the retention volume of unretained tracer, usually assumed to be that of the smallest injected molecule (in this work was used TTBB), V is the geometrical volume of the bed, Q is the flow rate of the mobile phase along the column and t_R is retention time of the unretained tracer at a given flow rate. The length of the preparative column, L is 10.1 cm and volume of the bed, V is 53.62×10^{-3} dm^3.

The chromatographic peaks for unretained tracer (TTBB) were obtained at flow rates from 5 cm^3/min to 40 cm^3/min using mixture of Heptane/2-propanol (95/5) as a mobile phase. The plot of reciprocal value of the retention time as a function of flow rate is shown in Fig. 3. The total porosity was obtained from the slope of the straight-line of the plot ($b = 1/\varepsilon_T V_b$). The obtained value of total porosity of preparative column packed with chiral adsorbent is 0.61.

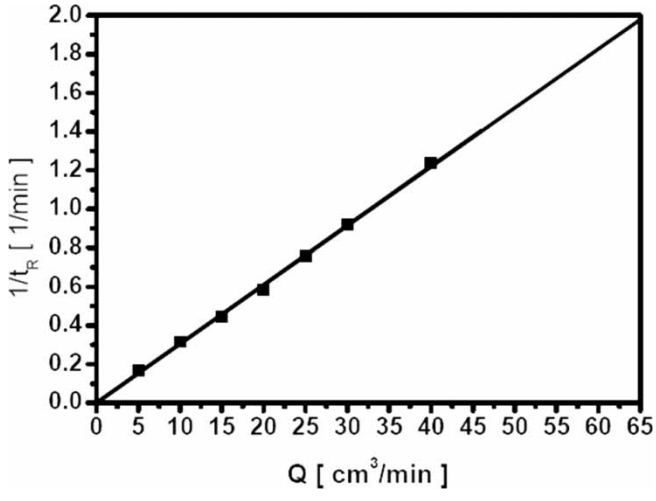

Figure 3. The plot of reciprocal retention time ($1/t^R$) versus flow rate (Q) for TTBB.

The permeability (B_0) value of the chiral column can be calculated using Darcy's law for laminar flow (8, 19, 20):

$$\frac{\Delta P}{L} = \frac{\eta}{B_0} u_0 \tag{15}$$

where u_0 is superficial velocity, η is viscosity of the mobile phase, L is length of the bed and ΔP is the column pressure drop.

The permeability of the bed is proportional to the square of particle diameter for laminar flow regime:

$$B_0 = \frac{\varepsilon^3 d_p^2}{36 h_k (1-\varepsilon)^2} \tag{16}$$

where d_p is the particle diameter, ε is the bed porosity, which was assumed to be equal 0.4 and h_k is the shape factor (for packing of uniform sphere, $h_k \cong 5$). The value of permeability was calculated from the experimental plots of pressure drop, ΔP versus the superficial velocity, u_0 shown in Fig. 4. The values of the pressure drop ΔP were obtained with an analytical column packed with the same adsorbent and dimensions 25 cm length and 0.46 cm diameter. This step was included due to hardware limitation of HPLC system. Since the permeability is a function of the particle diameter and external porosity of the column, the value of permeability obtained using the analytical column is considered as the permeability of the preparative column. The calculated value of permeability is 4.4×10^{-13} m^2.

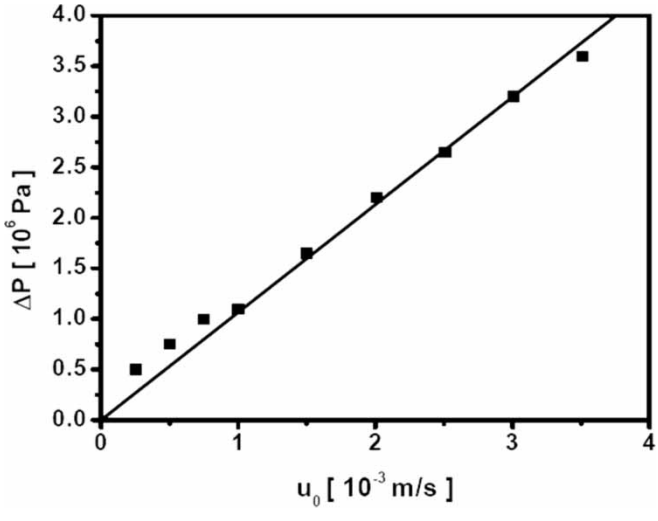

Figure 4. Pressure drop (ΔP) versus velocity through the bed of analytical column packed with CHIRALPAK AD.

Analysis of HETP Versus Flow Rate

The effect of fluid velocity on the equivalent height of a theoretical plate of pure enantiomers of R,S-α-Tetralol was measured. The efficiency of a column was characterized by the height equivalent to a theoretical plate (HETP). The HETP as a function of superficial velocity is calculated for each compound from the experimental chromatographic peak by the following equation:

$$HETP = \sigma^2 L/\mu_1^2 \tag{17}$$

where σ^2 is the peak variance and μ_1 is the first moment of the peak calculated as:

$$\mu_k = \int_0^\infty t^k C(t)\, dt \; k = 0, 1, 2, \ldots \tag{18}$$

$$\sigma^2 = \mu_2 - \mu_1^2 \tag{19}$$

where $C(t)$ is the experimental concentration history and L is length of bed.

Van Deemter derived the dependency of HETP on flow rate (12, 21):

$$HETP = A + \frac{B}{u_0} + Cu_0 \tag{20}$$

where A is the eddy diffusion term, B is a term that is reflecting the contribution of molecular diffusion and C is the term for mass transfer resistance.

In the tested range of flow rate, the dependence of plate height upon the velocity was linear and the term of molecular diffusion has not been considered, as its influence on the HETP curve under common HPLC condition was not observed. The Eq. (20) has been simplified as follows:

$$HETP = A + Cu_0 = ad_p + cd_p^2 u_0 \tag{21}$$

where the eddy diffusion term, A, is proportional to the particle size and the term for mass transfer resistance, C, is proportional to the square of particle diameter and u_0 is the superficial velocity of the solvent through the bed.

The plot of HETP curves of 1,3,5-Tri-tert-butylbenzene and pure enantiomers of R,S-α-Tetralol is reported in Fig. 5 and Fig. 6, respectively. The parameters of simplified van Deemter equation obtained by fitting experimental HETP points are reported in Table 2. The quality of the fit was also characterized by the correlation coefficient R^2 and sum of squares of differences (SSR) between the experimental and calculated data. The equation for the sum of squared differences is $SSR = \sum(x - y)^2$ where x is the first array or range of values and y is the second array or range of values.

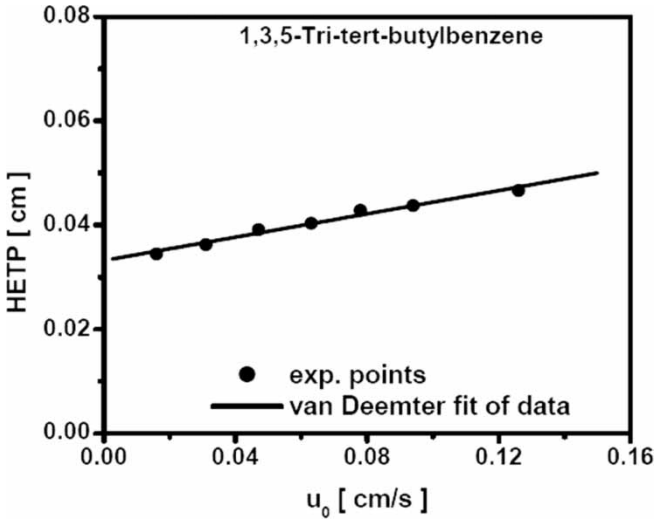

Figure 5. Experimental and calculated HETP for 1,3,5-Tri-tert-butylbenzene as a function of flow rate on the preparative column packed with CHIRALPAK AD.

The reciprocal retention time of both pure enantiomers of R,S-α-Tetralol as a function of the flow rate is shown in Fig. 7. The plot is a straight-line with the slope

$$\frac{1}{V(\varepsilon_T + (1-\varepsilon)K)} \tag{22}$$

where K is the initial slope of the linear isotherm. The retention times of both enantiomers were corrected for the dead time of the system. The obtained values for the initial slope of the isotherm for S-α-Tetralol and R-α-Tetralol are 2.96 and 3.46, respectively. The separation factor under linear condition, α, is defined as a ratio of the initial slopes for the more retained enantiomer and less retained enantiomer and is equal to 1.17.

Thermodynamics of Enantioseparation of S,R-α-Tetralol

The separation of the S and R enantiomers on the chiral stationary phases involves the reversible formation of a pair of reversible diastereomeric complexes between the species and the chiral stationary phase. These diastereomeric complexes must therefore differ adequately in free energy for an enantiomer separation to be observed (22).

The Gibbs free energy ΔG is related to the equilibrium constant K by:

$$\Delta G = \Delta H - T\Delta S = -RT \ln K \tag{23}$$

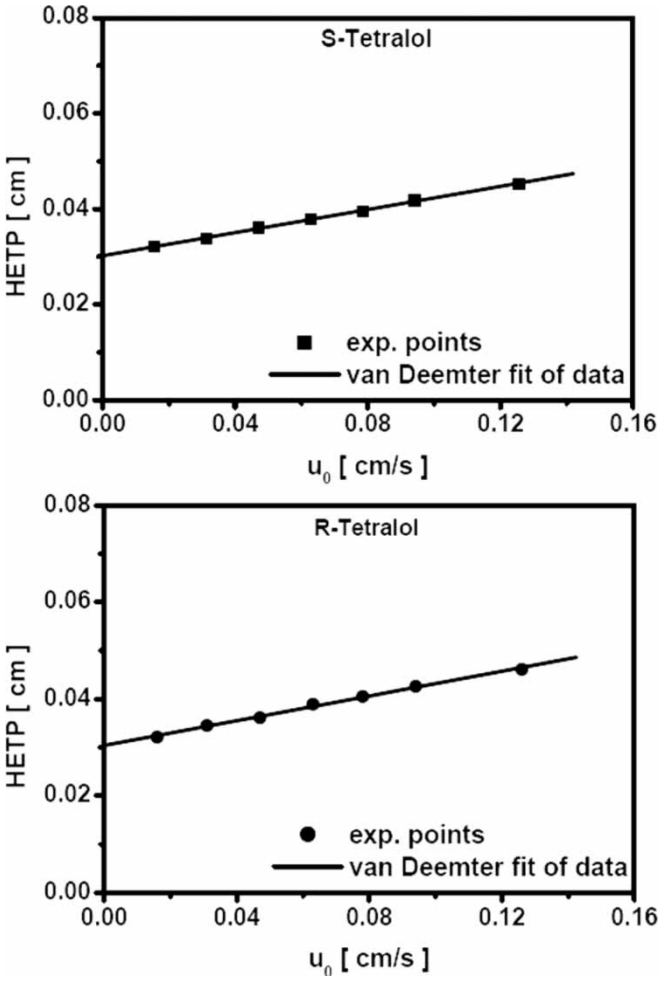

Figure 6. Experimental and calculated HETP for pure enantiomers of R,S-α-Tetralol as a function of flow rate on the preparative column packed with CHIRALPAK AD.

Table 2. Summary of the van Deemter parameters estimated for 1,3,5-Tri-tert-butylbenzene and the pure enantiomers of R,S-α-Tetralol

Compounds	*A*	*C*	SSR	R^2
1,3,5-Tri-tert-butylbenzene	0.033 ± 0.0008	0.1037 ± 0.0099	1.1×10^{-5}	0.9978
S-α-Tetralol	0.0302 ± 0.0002	0.1212 ± 0.0021	1.8×10^{-7}	0.9984
R-α-Tetralol	0.0304 ± 0.0003	0.1278 ± 0.0037	5.7×10^{-7}	0.9960

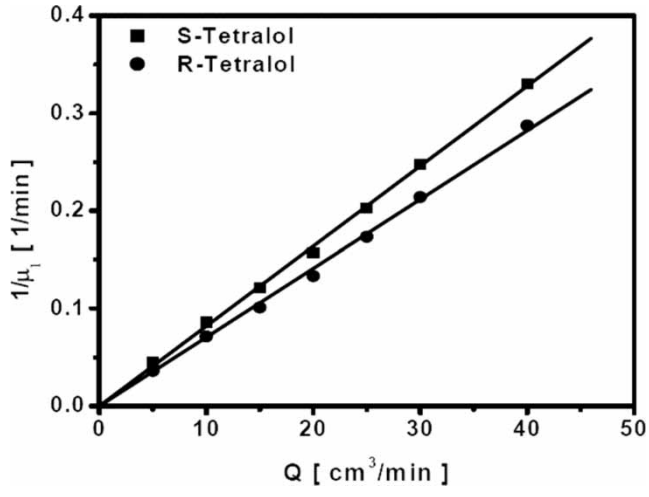

Figure 7. Effect of flow rate to the reciprocal values of retention time of both enantiomers of R,S-α-Tetralol on the preparative column filled with CHIRALPAK AD $d_p = 20$ μm.

and adsorption constant under linear condition, K, is related to the retention factor, k by: $k = \beta K$, where β is the phase ratio, $\beta = 1 - \varepsilon/\varepsilon$ and ε is the external porosity of the chromatographic column, respectively. Furthermore, enthalpy and entropy of transfer of solute from the mobile to the stationary phase can be determined from retention data by evaluation of the van't Hoff plots. The retention factor, k, can be expressed in terms of standard enthalpy and entropy by:

$$\ln k = -\frac{\Delta H}{RT} + \frac{\Delta S}{R} + \ln \beta \tag{24}$$

The enthalpy, ΔH, represents the measure of energy exchange. Entropy, ΔS, represents the chaos of a system and β is the phase ratio. If the van't Hoff plot is linear the enthalpy of transfer of solute from the mobile phase to the stationary phase, ΔH, and the entropy of transfer of solute from the mobile phase to the stationary phase, ΔS, are independent of the temperature over the temperature range investigated. The van't Hoff plot was not linear on the whole range of temperature tested, and therefore the thermodynamic parameters have been calculated from the linear part of van't Hoff plot. Nonlinearity of van't Hoff plot could indicate changes in the retention mechanism (23, 24).

As it was mentioned in the previous section the external porosity for the preparative column packed with chiral adsorbent was assumed as 0.4. From the slope and the intercept of the van't Hoff plot, the enthalpy of transfer and the standard entropy of transfer were calculated, respectively. The obtained

thermodynamic parameters are reported in Table 3. All thermodynamic experiments with chiral adsorbent CHIRALPAK AD were performed on the same system as discussed before. Experiments were performed at a flow rate of 5.0 cm^3/min and at temperatures of 5, 10, 15, 20, 27, 30, and 35°C. For every temperature change the column, with the mobile phase flowing through it, was equilibrated for half an hour at the desired temperature. The retention time of each peak of racemate of S,R-α-Tetralol were calculated from the peak maximum. The retention factor was determined as: $k = t_R - t_0/t_0$, where t_R is the retention time of one the enantiomers and t_0 is the retention time of inert tracer. The separation factor, α is given by: $\alpha = k_2/k_1$, where k_2 is the retention factor of the late eluting compound.

The values for the thermodynamic parameters: Gibbs free energy difference Δ(ΔG), enthalpy change Δ(ΔH) and entropy change Δ(ΔS) for the separation of the enantiomers were obtained from the plot of the natural logarithm of separation factor (ln α) against the reciprocal of the column absolute temperature (1/T). The relationship between the enantioselectivity and Gibbs energy is given by (22, 25, 26)

$$\ln \alpha = -\Delta(\Delta G)/RT = -\frac{\Delta_{RS}(\Delta H)}{RT} + \frac{\Delta_{RS}(\Delta S)}{R} \tag{25}$$

The influence of the column temperature on the retention is summarized by the van't Hoff plot in Fig. 8. The plot is not reported for the whole range of temperature, but only for the range from 5°C up to 27°C. As can be seen from the predicted line the retention of the analyte decreases as the column temperature was increased. It may be said that with increasing temperature the analytes have smaller adsorption and the migration through the column is faster. The plot of the separation factor, α, versus absolute temperature (278–308 K) is shown in Fig. 9.

The enantioselectivity of the column is increasing with increasing column temperature until 300 K. It may be said, there are different mechanisms operating on the CHIRALPAK AD. The plot of the separation factor, α, versus temperature of the column is not linear on the whole range of

Table 3. Thermodynamic parameters of enantioseparation

Compound	S-α-Tetralol		R-α-Tetralol
Temp. range (°C)		5 → 27	
$-\Delta H$ [J/mol]	1925.2		1639.6
$-\Delta_{RS}\Delta H$ [J/mol]		−285.6	
ΔS [J/mol K]	−2.66		−0.75
$\Delta_{RS}\Delta S$ [J/mol K]		1.91	
$-\Delta G_{27°C}$ [J/mol]	1126.8		1414.5
$-\Delta_{RS}\Delta G_{27°C}$ [J/mol]		287.7	
R^2	0.993		0.996

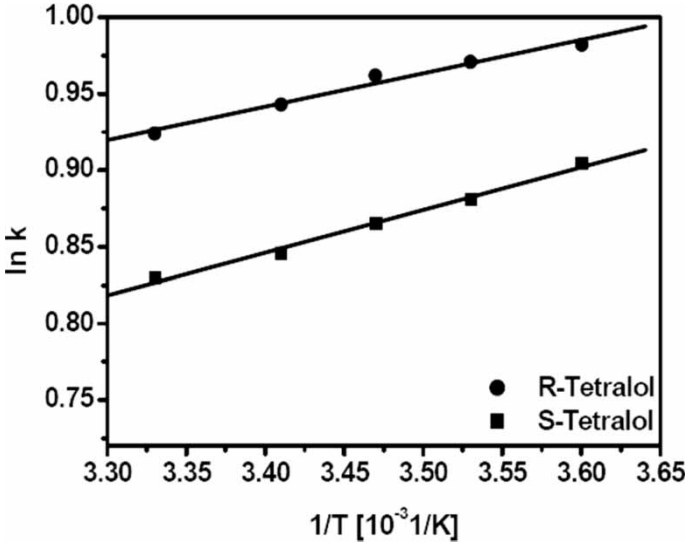

Figure 8. The van't Hoff plot for the enantioseparation of S,R-α-Tetralol on CHIRALPAK AD (dp = 20 μm).

column temperature and therefore only the linear part of the plot was used to evaluate the thermodynamic parameters. The plot of ln α versus reciprocal absolute temperature on the range from 5°C to 27°C is reported in Fig. 10 and the evaluated parameters are listed in Table 3.

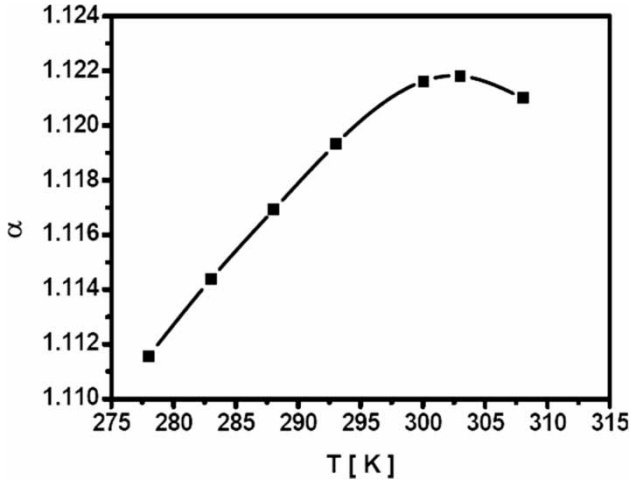

Figure 9. Plot of the separation factor of S,R-α-Tetralol enantiomers,α, versus absolute temperature (temperature range: 278 K – 308 K).

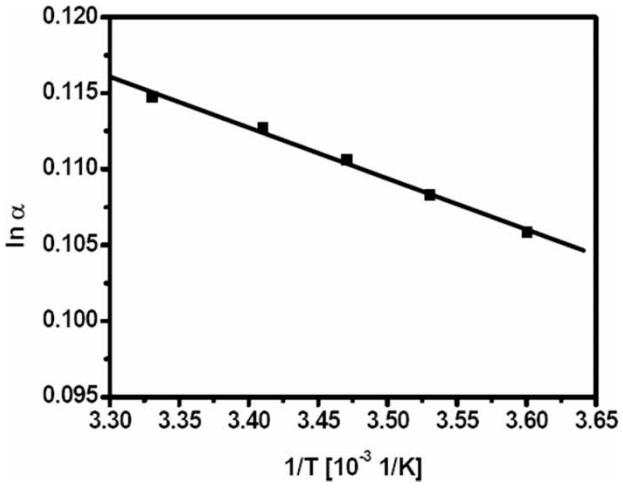

Figure 10. The plot of lnα versus 1/T (temperature range: 278 K – 300 K).

Determination of Single and Competitive Component Isotherms

Among the various chromatographic methods available to determine competitive isotherms, frontal analysis is the most accurate (9, 27, 28). Competitive isotherms were experimentally determined for the separation of chiral alcohol R,S-α-Tetralol. It consists in quickly replacing the stream of mobile phase percolating through the column with solutions of the studied compounds of increasing concentrations and recording the breakthrough curves at the column outlet.

The adsorbed amount of each enantiomer was calculated from desorption after the bed was saturated with a given feed concentration of racemic mixture The whole desorbed volume was collected and sample of it was analyzed. Mass balance is given:

$$V_e c_i^e = \varepsilon_T V c_{i,f} + (1 - \varepsilon) V q_{i,f}^* \tag{26}$$

where the concentration of each component retained in the adsorbent, $q_{i,f}^*$, in equilibrium with the feed concentration, $c_{i,f}$ [g/dm^3], of each of the compounds in the mobile phase, c_i^e [g/dm^3], is the concentration of species i in the desorbed volume, V_e [dm^3], V [dm^3] is the column volume and ε is the bed porosity, and ε_T is the total porosity. The total loading capacity for each concentration was calculated so that a point of the adsorption isotherm was obtained.

The competitive adsorption isotherm was determined in the concentration range from 1 g/dm^3 to 16 g/dm^3 of racemic mixture and shown in Fig. 11. The adsorbed amount, $q_{\mathrm{i,f}}^*$ [g/dm^3 of adsorbent], of the solute in the stationary phase at equilibrium with a given concentration, $c_{i,f}$ [g/dm^3], in the mobile phase was calculated according to the Eq. (26.) The non-linear competitive isotherms were obtained in the whole range of tested concentration.

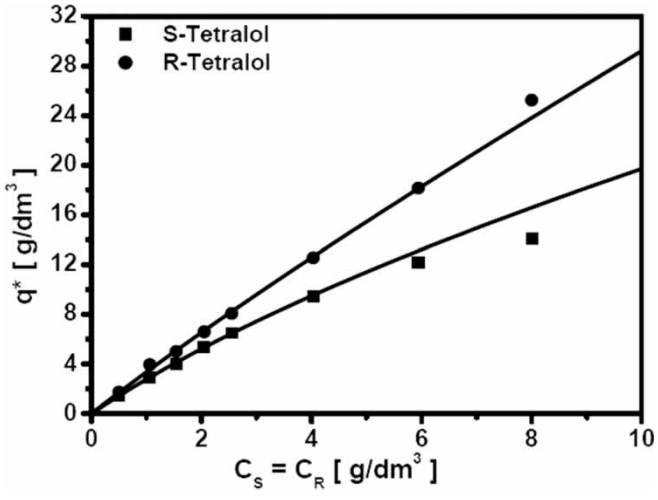

Figure 11. Competitive adsorption isotherm for the R,S-α-Tetralol on the CHIRALPAK AD with particle size 20 μm at a temperature 25°C.

Racemic solutions were used for adsorption equilibrium isotherm measurements.

When enantiomers are separated on a chiral stationary phase, the stationary phase is usually heterogeneous. There are selective sites of the adsorbent where each of the enantiomers interacts differently and nonselective sites retain the enantiomers identically. To model adsorption on heterogeneous surfaces, several appropriate multicomponent isotherm models were investigated (28). However, most of these multicomponent adsorption isotherms account for the competition between species for the available selective sites but generally fail when the selectivity is concentration dependent. Concentration dependent selectivity can be simply described by the linear + Langmuir isotherm model, which has been previously used to characterize the adsorption isotherm on chiral stationary phases (29–32). The adsorption equilibrium isotherm equation for the species i and j is given by:

$$q_i^* = Hc_i + \frac{q_s b_i c_i}{1 + b_i c_i + b_j c_j} \tag{27}$$

where $H[-]$ is the equilibrium constant for the adsorption of either enantiomers on the non-selective sites, b_i, b_j [dm^3/g] are equilibrium constants for the adsorption of enantiomers i (S-Tetralol), and j (R-Tetralol) on the enantioselective sites and q_s [g/dm^3] is the saturation capacity of the enantioselective sites. The saturation capacity of the enantioselective sites was assumed to be equal for both enantiomers.

The best-fitted parameters of the competitive adsorption equilibrium isotherms for S-α-Tetralol and R-α-Tetralol are reported in Eq. (28) a, b, respectively.

$$q_S^* = 1.14C_S + \frac{23.6 \cdot 0.077C_s}{1 + 0.077C_S + 0.042C_R} \tag{28a}$$

$$q_R^* = 2.47C_R + \frac{23.6 \cdot 0.042C_R}{1 + 0.077C_S + 0.042C_R} \tag{28b}$$

To obtain the parameters of the isotherm model with physical meaning and thermodynamically consistent, the adsorption constant, K_i, for each

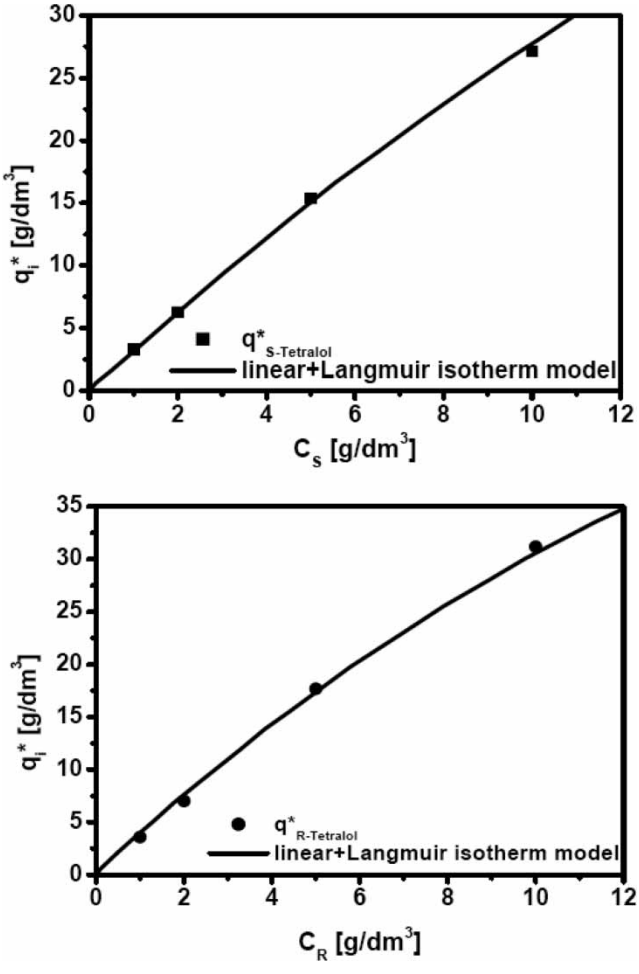

Figure 12. Single adsorption isotherm for the pure S-α-Tetralol and R-α-Tetralol on the analytical column packed with CHIRALPAK AD.

enantiomer under linear condition is given by $K_i = H_i + q_s b_i$, and are K_S is 2.96 and K_R is 3.46.

A single adsorption equilibrium isotherm for the pure S-α-Tetralol and R-α-Tetralol on the analytical column packed with CHIRALPAK AD at a temperature 25°C and at flow rate 1 ml/min was measured (see Fig. 12).

Validation of the Mathematical Model

The validity of the mathematical model including the multi-component linear + Langmuir isotherm was checked using experiments with different pulse period and also with breakthrough and desorption curves.

Pulse experiments and breakthrough and desorption curve experiments were carried out at a flow rate of 5.0 cm^3/min ± 0.2 cm^3/min and at a temperature of 25°C. The parameters of the mathematical model were calculated according to Eq. (7) to Eq. (13) and they are summarized in Table 4. The mathematical model includes the overall mass transfer coefficient Eq. (7) and is obtained from external Eq. (10) and internal Eq. (8) mass transfer resistances. As can be seem from Table 4, the intraparticle transport is about one order of magnitude slower than external mass transfer and therefore is the rate-limiting step and the influence of the external mass transfer is negligible.

Experimental and simulated pulse responses at total feed concentration 5 g/dm^3 of the preparative column packed with pulse duration 1 minute and

Table 4. Parameters used in the mathematical model

Parameters	CHIRALPAK AD $d_p = 20$ μm
Q [cm^3/min]	5
d_p [cm]	2.7×10^{-3}
L [cm]	10.1
ε_T	0.61
ε	0.4
ε_i	0.35
τ	7.8
Re	0.0064
Sc	238
Sh	3.12
D_m [cm^2/s]	2.8×10^{-5}
D_L [cm^2/s]	5.3×10^{-5}
k_{ext} [cm/s]	0.032
k_{int} [cm/s]	0.0047
k_{ov} [cm/s]	0.0041
$\rho = 0.689$ cm^3/g	$\eta = 0.45 \times 10^{-3}$ Pa · s

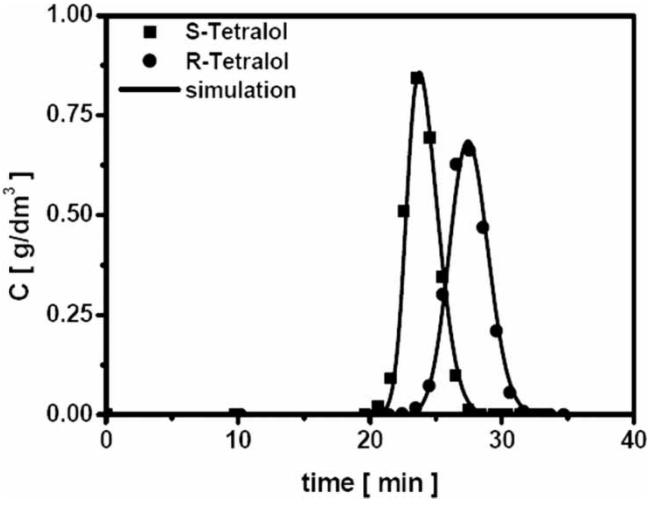

Figure 13. Pulse response of the column CHIRALPAK AD at total feed concentration 5 g/dm^3 of racemic mixture and pulse duration 1 minute.

5 minutes are shown in Figs. 13 and 14, respectively. Good agreement between the simulated and experimental pulse profile was found.

A comparison between experimental and simulated breakthrough curves and desorption curves of R,S-α-Tetralol obtained on column packed with CHIRALPAK AD at a concentration of racemic mixture 1 g/dm^3 2 g/dm^3, 8 g/dm^3 and 12 g/dm^3 are presented in Figs. 15–18, respectively.

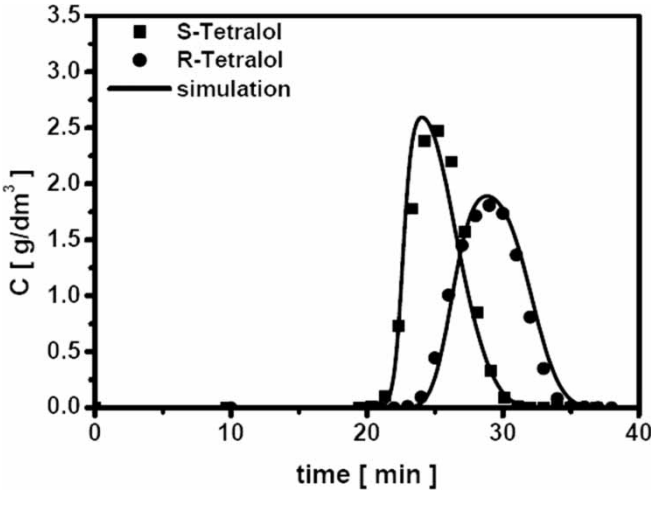

Figure 14. Pulse response of the column CHIRALPAK AD at total feed concentration 5 g/dm^3 of racemic mixture and pulse duration 5 minute.

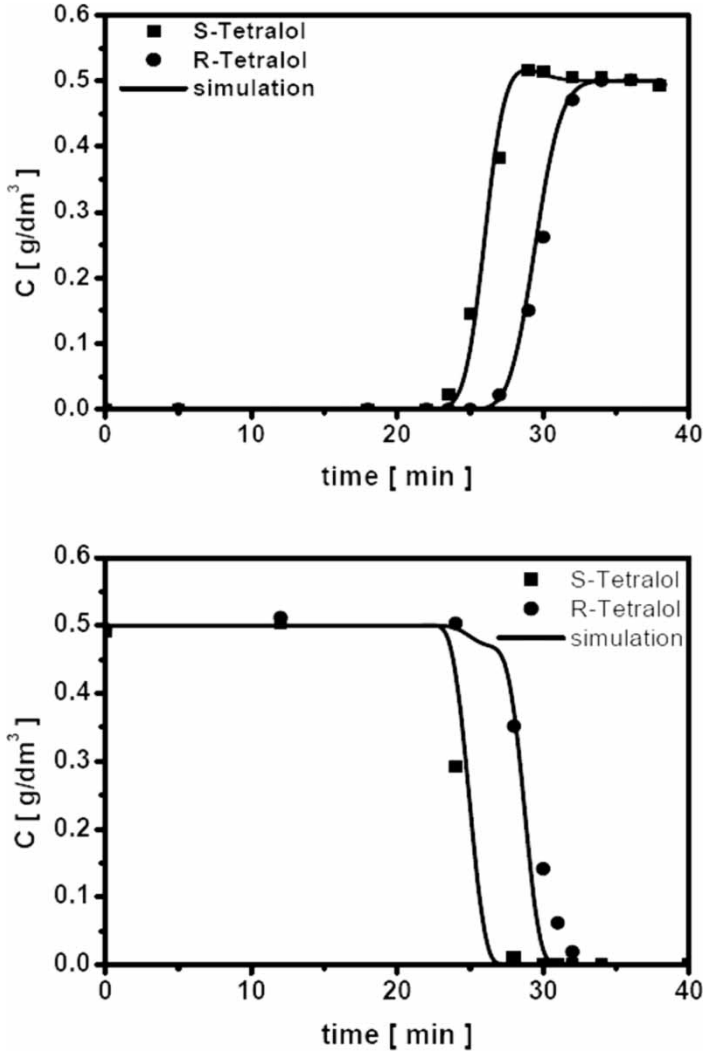

Figure 15. Breakthrough curves and desorption curves of racemic mixture on the chiral adsorbent CHIRALPAK AD (Total feed concentration: 1 g/dm^3).

Good agreement between the experimental (symbols) and simulated (solid line) profiles were found for the breakthrough curves and desorption curves of the enantiomers of R,S-α-Tetralol onto chiral adsorbent CHIRALPAK AD at total feed concentration 1 g/dm^3, 2 g/dm^3, 8 g/dm^3 using a multicomponent linear + Langmuir isotherm model and proposed mathematical model.

Some disagreement can be found at total feed concentration 12 g/dm^3 (Fig. 18). This could be caused by higher inaccuracy between the experimental points and the predicted adsorption equilibrium isotherm model. On the other

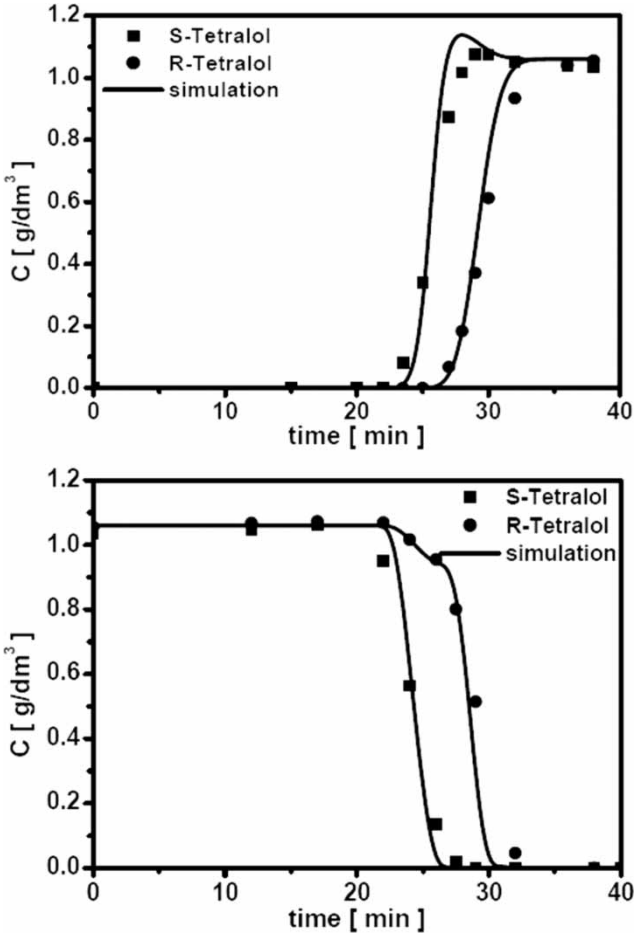

Figure 16. Breakthrough curves and desorption curves of racemic mixture on the chiral adsorbent CHIRALPAK AD (Total feed concentration: 2 g/dm^3).

hand, through these experiments a strong retention of more retained species (R-α-Tetralol) was observed in desorption curves after the bed was saturated with these total feed concentrations. In these cases, the adsorption equilibrium isotherm parameters failed to describe the behavior of these species.

In order to verify the mass balance on the adsorption and desorption part of the wide rectangular pulses the adsorbed amount, q_i^*, of the species were calculated. The obtained values adsorbed amount, q_i^*, are compared with the isotherm fitting using Eq. (28 a,b) in Fig. 19. One can observe large error (approximately 20%) at high total feed concentration (>8 g/dm^3). Although some part of the error in mass balance on the adsorption and the desorption part of the wide rectangular pulse is caused by inaccurate integration of the area due to lack of the experimental points. On the other hand, it should be pointed out that the major

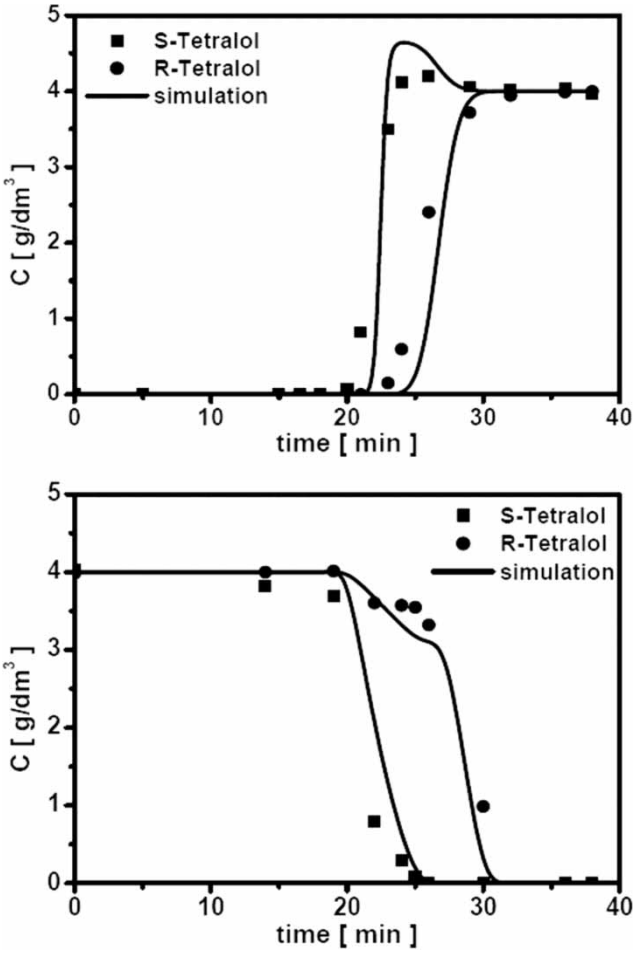

Figure 17. Breakthrough curves and desorption curves of racemic mixture on the chiral adsorbent CHIRALPAK AD (Total feed concentration: 8 g/dm^3).

part of this difference is caused by strong retention of more retained compounds in desorption. The reason for this behavior can be found looking on the strength of the mobile phase. Separation of the enantiomers of S,R-α-Tetralol has been previously reported by Ludemann-Hombourger (33) using the mobile phase with composition n-Heptane/2-propanol (95/5) and a small concentration of the trifluoroacetic acid used as acidic modifier. Acidic modifiers are used to minimize the interaction with residual silanols and improved the peak shape (34, 35). In our case, the acidic modifier trifluoroacetic acid was excluded with respect to the future separation of S,R-α-Tetralol using SMB chromatography, where the aim is to use the simplest mobile phase composition (36).

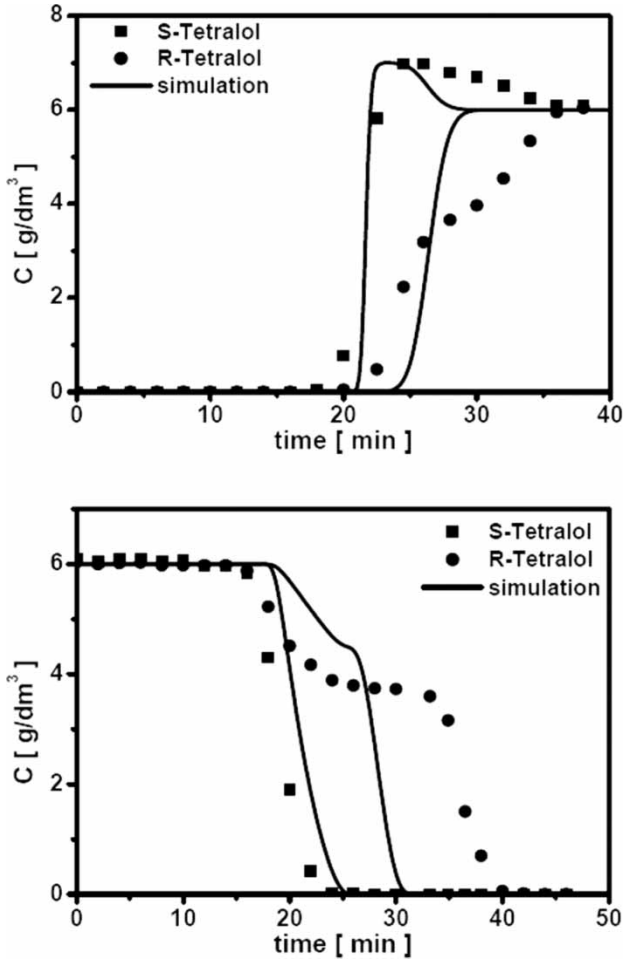

Figure 18. Breakthrough curves and desorption curves of racemic mixture on the chiral adsorbent CHIRALPAK AD (Total feed concentration: 12 g/dm^3).

CONCLUSIONS

The hydrodynamic properties of the preparative column packed with chiral adsorbent CHIRALPAK AD with particle size 20 μm have been evaluated. The mobile phase dependence of the height equivalent to a theoretical plate (HETP) and adsorption dynamics of the chiral adsorbent CHIRALPAK AD was studied.

The total porosity of the preparative column packed with CHIRALPAKAD with particle size 20 μm by using non-retained tracer (1,3,5-Tri-tert-butylbenzene)

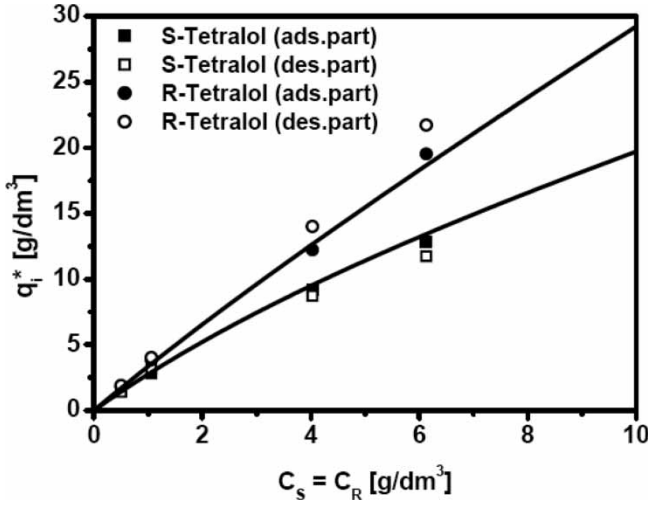

Figure 19. Comparison between fitting of the isotherm (Eq. 28 a, b) and the adsorbed amount, q_i^*, calculated from the breakthrough curve experiments.

were 0.61. The permeability of the bed packed with CHIRALPAK AD was calculated and is equal to 4.4×10^{-13} m^2.

The efficiency of the preparative column was characterized through the height equivalent to a theoretical plate (HETP) of each enantiomer of R,S-α-Tetralol. The HETP of the S-α-Tetralol and R-α-Tetralol at the flow rate 5.0 cm^3/min was 0.032 cm and 0.034 cm, respectively. The dependence in the tested range of flow rates used was linear.

The thermodynamic parameters enthalpy, ΔH and entropy, ΔS have been calculated from the van't Hoff plot for the temperature range from 5°C to 27°C. The calculated enthalpies ΔH of S-α-Tetralol and R-α-Tetralol are -1925.2 J/mol and -1639.6 J/mol, respectively. The calculated entropies, ΔS of S-α-Tetralol and R-α-Tetralol are -2.66 J/mol · K and -0.75 J/mol · K, respectively. It was shown that with increasing temperature, the analytes have smaller adsorption and the migration through the column was faster.

The multicomponent adsorption equilibrium isotherm of racemic mixture of R,S-α-Tetralol was measured. The linear + Langmuir model of the adsorption isotherm for the heterogeneous stationary phase was assumed. The parameters of the isotherms model are reported in Eq. (28) a,b. The initial slope of the isotherm for S-α-Tetralol and R-α-Tetralol are 2.96 and 3.46, respectively.

The mathematical model includes axial dispersion for the fluid flow and linear driving force for the intraparticle mass transfer. The mathematical model reasonably predicts pulse profiles with different time duration and also breakthrough and desorption curves of enantiomer of R,S-α-Tetralol.

NOMENCLATURE

B_0	permeability (m^2)
b	equilibrium constant for the adsorption of enantiomers (m^3/kg)
C	bulk liquid phase concentration (kg/m^3)
C_0	initial (feed) concentration (kg/m^3)
C_p	liquid concentration in the particle pores (kg/m^3)
$\bar{C}_p$	average liquid concentration in the particle pores (kg/m^3)
D_L	axial dispersion coefficient (m^2/s)
d_c	diameter of the column (m)
d_p	diameter of particle (m)
D_m	molecular diffusion (m^2/s)
D_p	pore diffusion (m^2/s)
H	adsorption equilibrium constants of non-selective site (−)
ΔH	enthalpy (J/mol)
ΔG	Gibbs free energy (J/mol)
K	adsorption equilibrium constants (−)
k_{ext}	external mass transfer coefficient (1/s)
k_{int}	internal mass transfer coefficient (1/s)
k_{ov}	overall mass transfer coefficient (1/s)
L	length of the column (m)
M	molecular weight of the solute (g/mol)
ΔP	column pressure drop (Pa)
q	adsorbed phase concentration (kg/m^3)
$\bar{q}_i$	average adsorbed phase concentration in particle (kg/m^3)
q^*	equilibrium adsorbed concentration (kg/m^3)
q_s	adsorbed phase saturation concentration of component (kg/m^3)
Re	Reynolds number (−)
ΔS	entropy (J/mol K)
Sc	Schmidt number (−)
Sh	Sherwood number (−)
Q	flow rate (m^3/s)
T	temperature (K)
t	time variable (s)
t_R	retention time (s)
u_0	superficial velocity (m/s)
ν	interstitial velocity (m/s)
V	volume of the bed (m^3)
V_e	elution volume (m^3)
V_m	molar volume of the adsorbate at its normal boiling temperature (m^3/mol)
V_T	retention volume non-adsorbed tracer (m^3)
x	molar fraction (−)
z	axial variable (m)

Greek Letters

α	selectivity factor (−)
ε	external porosity (−)
ε_p	internal porosity (−)
ε_T	total porosity (−)
ϕ	association factor (−)
η	viscosity (Pa.s)
μ_1	first moment of the peak (s)
ρ	fluid density (kg/m^3)
σ^2	peak variance (s^2)
τ	tortuosity (−)

Subscript and Superscript

i, j	species in binary system

ACKNOWLEDGMENTS

Michal Zabka (SFRH/BD/5418/2001) gratefully acknowledged the Ph.D grant from the "Fundação para a Ciência e Tecnologia."

Chiral Technologies Europe is gratefully acknowledged by supplying the chiral adsorbent.

REFERENCES

1. Caldwell, J. (1995) Stereochemical determinants of the nature and consequences of drug-metabolism. *J. Chromatogr. A*, 694 (1): 39.
2. Maier, N.M., Franco, P., and Lindner, W. (2001) Separation of enantiomers: needs, challenges, perspectives. *J. Chromatogr. A*, 906 (1–2): 3.
3. Francotte, E.R. (2001) Enantioselective chromatography as a powerful alternative for the preparation of drug enantiomers. *J. Chromatogr. A*, 906 (1–2): 379.
4. Oguni, K., Oda, H., and Ichida, A. (1995) Development of chiral stationary phases consisting of polysaccharide derivatives. *J. Chromatogr. A*, 694 (1): 91.
5. Zhang, T., Kientzy, C., Franco, P., Ohnishi, A., Kagamihara, Y., and Kurosawa, H. (2005) Solvent versatility of immobilized 3,5-dimethylphenylcarbamate of amylose in enantiomeric separations by HPLC. *J. Chromatogr. A*, 1075 (1–2): 65.
6. Zhang, T., Nguyen, D., Franco, P., Murakami, T., Ohnishi, A., and Kurosawa, H. (2006) Cellulose 3,5-dimethylphenylcarbamate immobilized on silica—A new chiral stationary phase for the analysis of enantiomers. *Anal. Chim. Acta*, 557 (1–2): 221.
7. Ali, I. and Aboul-Enein, H.Y. (2006) Impact of immobilized polysaccharide chiral stationary phases on enantiomeric separations. *J. Sep. Sci.*, 29 (6): 762.

8. Ruthven, D.M. (1984) *Principles of Adsorption and Adsorption Processes*. Wiley: New York.
9. Guiochon, G., Shirazi, S.G., and Katti, A.M. (1994) *Fundamentals of Preparative and Nonlinear Chromatography*; Academic press: Boston.
10. Santacesaria, E., Morbidelli, M., Servida, A., Storti, G., and Carra, S. (1982) Separation of xylenes on y-zeolites.2. Breakthrough curves and their interpretation. *Ind. Eng. Chem. Process. Des. Dev.*, 21 (3): 446.
11. Silva, V. and Rodrigues, A.E. (2002) Dynamics of a fixed-bed adsorptive reactor for synthesis of diethylacetal. *AIChE J.*, 48 (3): 625.
12. Horvath, C. and Lin, H.-J. (1978) Band spreading in liquid chromatography: General plate height equation and a method for the evaluation of the individual plate height contributions. *J. Chromatogr. A*, 149: 43.
13. Wilke, C.R. and Chang, P. (1955) Correlation of diffusion coefficients in dilute solutions. *AIChE J.*, 1 (2): 264.
14. Perkins, L.R. and Geankoplis, C.J. (1969) Molecular diffusion in a ternary liquid system with diffusing component dilute. *Chem. Eng. Sci.*, 24 (7): 1035.
15. Teja, A.S. and Rice, P. (1981) Generalized corresponding states method for the viscosities of liquid-mixtures. *Ind. Eng. Chem. Fundam.*, 20 (1): 77.
16. Reid, R.C., Prausnitz, J.M., and Poling, B.E. (1987) *Properties of Gas and Liquids*; McGraw Hill: New York.
17. gPROMS, *gPROMS v2.2 User Guide*; 2003, Process System Enterprise Ltd.
18. Nicoud, R.M. (1993) A packing procedure suitable for high flow rate and high stability columns using cellulose triacetate. *LC-GC Int.*, 6: 636.
19. Rodrigues, A.E., Chenou, C., and delaVega, M.R. (1996) Protein separation by liquid chromatography using permeable POROS Q/M particles. *Chem. Eng. J. & Biochem. Eng. J.*, 61 (3): 191.
20. de la Vega, M.R., Chenou, C., Loureiro, J.M., and Rodrigues, A.E. (1998) Mass transfer mechanisms in Hyper D media for chromatographic protein separation. *Biochem. Eng. J.*, 1 (1): 11.
21. Van Deemter, J., Zuiderweg, F., and Klinkenberg, A. (1956) Longitudinal diffusion and resistance to mass transfer as causes of nonideality in chromatography. *Chem. Eng. Sci.*, 5 (6): 271.
22. Cabusas, M.E.Y. (1998) Chiral separation on HPLC derivatized polysaccharide CSPs: Temperature, mobile phase and chiral regocnition mechanism studies. Ph.D. Thesis, Virginia Polytechnic Institute: Blacksburg.
23. Lamparczyk, H. and Zarzycki, P.K. (1995) Effect of temperature on separation of estradiol stereoisomers and equilin by liquid-chromatography using mobile phases modified with beta-cyclodextrin. *J. Pharm. Biomed. Anal.*, 13 (4–5): 543.
24. Peter, A., Torok, G., Armstrong, D.W., Toth, G., and Tourwe, D. (1998) Effect of temperature on retention of enantiomers of beta-methyl amino acids on a teicoplanin chiral stationary phase. *J. Chromatogr. A*, 828 (1–2): 177.
25. Seidel-Morgenstern, A. and Guiochon, G. (1993) Thermodynamics of the adsorption of troger base enantiomers from ethanol on cellulose triacetate. *J. Chromatogr. A*, 631 (1–2): 37.
26. Trapp, O. and Schurig, V. (2001) Approximation function for the direct calculation of rate constants and Gibbs activation energies of enantiomerization of racemic mixtures from chromatographic parameters in dynamic chromatography. *J. Chromatogr. A*, 911 (2): 167.
27. Seidel-Morgenstern, A. (2004) Experimental determination of single solute and competitive adsorption isotherms. *J. Chromatogr. A*, 1037 (1–2): 255.

28. Nicoud, R.M. and Seidel-Morgenstern, A. (1996) Adsorption isotherm: Experimental determination and application to preparative chromatography. *Isol. & Purif.*, 2: 165.
29. Rodrigues, A.E., Lu, Z.P., Loureiro, J.M., and Pais, L.S. (1995) Separation of enantiomers of 1a,2,7,7a-tetrahydro-3-methoxynaphtha-(2,3b)-oxirane by liquid-chromatography — laboratory-scale elution chromatography and modeling of simulated moving-bed. *J. Chromatogr. A*, 702 (1–2): 223.
30. Charton, F. and Nicoud, R.M. (1995) Complete design of a simulated moving-bed. *J. Chromatogr. A*, 702 (1–2): 97.
31. Pais, L.S., Loureiro, J.M., and Rodrigues, A.E. (1998) Separation of enantiomers of a chiral epoxide by simulated moving bed chromatography. *J. Chromatogr. A*, 827 (2): 215.
32. Pais, L.S. and Rodrigues, A.E. (2003) Design of simulated moving bed and Varicol processes for preparative separations with a low number of columns. *J. Chromatogr. A*, 1006 (1–2): 33.
33. Ludemann-Hombourger, O., Nicoud, R.M., and Bailly, M. (2000) The "VARICOL" process: A new multicolumn continuous chromatographic process. *Sep. Sci. Technol.*, 35 (12): 1829.
34. Blackwell, J.A., Stringham, R.W., and Weckwerth, J.D. (1997) Effect of mobile phase additives in packed-column subcritical and supercritical fluid chromatography. *Anal. Chem.*, 69 (3): 409.
35. Stringham, R.W. and Ye, Y.K. (2006) Chiral separation of amines by high-performance liquid chromatography using polysaccharide stationary phases and acidic additives. *J. Chromatogr. A*, 1101 (1–2): 86.
36. Schulte, M., Ditz, R., Devant, R.M., Kinkel, J.N., and Charton, F. (1997) Comparison of the specific productivity of different chiral stationary phases used for simulated moving-bed chromatography. *J. Chromatogr. A*, 769 (1): 93.